

## Social-ecological modelling of the spatial distribution of dengue fever and its temporal dynamics in Guayaquil, Ecuador for climate change adaption

Gabriel Jácome<sup>a,b</sup>, Paulina Vilela<sup>a,c</sup>, ChangKyoo Yoo<sup>a,\*</sup>

<sup>a</sup> Department of Environmental Sciences and Engineering, College of Engineering, Center for Environmental Studies, Kyung Hee University, Seocheon-dong 1, Giheung-gu, Yongin-si, Gyeonggi-do 446-701, Republic of Korea

<sup>b</sup> Escuela de Recursos Naturales Renovables, Facultad de Ingeniería en Ciencias Agropecuarias y Ambientales, Universidad Técnica del Norte (UTN), Avenida 17 de Julio 5-21, y Gral José María Cordova, EC100150 Ibarra, Ecuador

<sup>c</sup> ESPOL Polytechnic University, Escuela Superior Politécnica del Litoral, ESPOL, Facultad de Ingeniería en Ciencias de la Tierra, Campus Gustavo Galindo Km. 30.5 Vía Perimetral, P.O. Box 09-01-5863, Guayaquil, Ecuador



### ARTICLE INFO

#### Keywords:

Dengue fever  
Social and ecological model  
Spatial distribution  
*Aedes aegypti*  
Ecuador  
Climate change adaption

### ABSTRACT

Researchers have showed that climatic, population, economic, and social characteristics contribute to the proliferation of *Aedes aegypti*, the main vector of dengue fever (DF) in Ecuador. In this study, we identified the factors with the greatest influence on dengue virus spread using a spatio-temporal analysis. We applied the maximum entropy algorithm (MaxEnt) to determine the spatial distribution of DF and identify areas with high probability of presence of *A. aegypti* by analyzing monthly climatic conditions, locations of reported dengue cases during 2012, and social factors in Guayaquil. Social variables showed greater influence on the presence and spread of disease during dengue outbreak season. The best model performance was obtained when the most important social variables were grouped based on components of the population's unsatisfied basic needs (UBN). Head of the household was a woman, the household was unoccupied, and UBN related to housing conditions at the household level were the most significant social risk factors. The final spatial distribution shows that the districts with the highest risks of infection are located mainly in the southern portion of the city, therefore these areas must take priority when integrated vector-control interventions and prevention protocols are carried out.

### 1. Background

Dengue fever (DF) is a disease that dispersed worldwide in the tropics during the 18th and 19th centuries (Gubler, 2002). The World Health Organization estimates that about 100 million DF infections occur annually, and that approximately 2.5 billion people live in countries where dengue is endemic (WHO, 2012; Real-Cotto et al., 2017). The mosquito *Aedes aegypti* is the main vector of DF in the neotropical region, being widely associated with human settlements and water storage practices that provide habitats for larval development (Cardoso-Leite et al., 2014). In Ecuador, DF has exhibited endemic-epidemic behavior since its appearance in 1988. Since then, several epidemic cycles have occurred progressively associated with vector dispersion (Real-Cotto et al., 2017). The Ministry of Public Health of Ecuador states that the persistence of disease transmission is associated with social, economic, and environmental factors that are present in approximately 70% of the national territory, and that 8,220,000 inhabitants might be at risk of infection (Ministerio de Salud

Pública del Ecuador, 2013; Stewart-Ibarra et al., 2013). Currently, dengue transmission is endemic throughout the year in Ecuador, and epidemic cycles usually coincide with the rainy season in places where conditions are favorable to accelerated vector reproduction (Ministerio de Salud Pública del Ecuador, 2013; OMS, 2009).

Factors influencing the occurrence and spread of DF epidemics vary depending on the geographic area being studied and the climatic, cultural, and socioeconomic characteristics of that region (Johansson et al., 2009; Reiter, 2001). Due to the importance of climatic and social aspects to disease spread, studies have identified risk factors at the city scale, and that mosquito presence is associated with human behavior and poverty-related issues that affect quality of life (Lippi et al., 2018; Stewart-Ibarra et al., 2014; Teurlai et al., 2015). The effects of socio-environmental variables on dengue transmission and on dengue vectors are often not immediate, since the lag between exposure to a risk factor and development of the disease are decisive aspects (Racloz et al., 2012). For this reason, the predictive accuracy studies must include both spatial and temporal aspects, and yield results that allow the

\* Corresponding author.

E-mail address: [ckyoo@knu.ac.kr](mailto:ckyoo@knu.ac.kr) (C. Yoo).

identification of areas at high risk of infection as well as the temporal kinetics of an outbreak season, all in a single model. The aim of such studies is to provide valuable information regarding proper control measures to be executed throughout the year (Wen et al., 2006). Recently, mathematical models have been implemented using geographic information system data to identify zones with the greatest probability of vector presence (Cardoso-Leite et al., 2014; Fischer et al., 2014; Khormi and Kumar, 2014; Kraemer et al., 2015; Masimalai, 2015; Fatima et al., 2016; Koch et al., 2016) and therefore DF occurrence.

In this research, we developed a social-ecological spatial and temporal model of DF in Guayaquil, Ecuador describing each month of one year using a species distribution model. Our aim was to compare an ecological model (EM), which includes climatic variables, with a social-ecological model (SEM) to which anthropogenic factors were added. In the species distribution models, records of vector presence and environmental variables were integrated in the context of probability-of-occurrence to identify spatial distribution patterns (Cardoso-Leite et al., 2014; Fatima et al., 2016; Fischer et al., 2014; Moya et al., 2017). Our results demonstrate the influence of social variables on model accuracy and identified factors that are essential to describe the disease dynamics and ecology of *A. aegypti* at the city scale. This analytical strategy makes it possible to evaluate the variability of the probability of DF occurrence throughout the year on a monthly basis as well as in total and general perspectives. Our analysis of variable importance showed that factors associated with the concept of unsatisfied basic needs (UBN) (Feres and Mancero, 2001) are the most influential variables affecting model performance. Therefore, we suggest grouping these social factors to create indexes that may be used as input data and to eliminate collinearity issues and improve the performance of species distribution model to produce a more accurate risk map. This approach can provide helpful information to health agencies for the design of public health interventions, vector control activities, and surveillance systems (Heydari et al., 2017; Stewart-Ibarra et al., 2014). Such information can assist in the assignment of resources to priority zones, in the forecasting of vector establishment, and the identification of vector habitat (Cardoso-Leite et al., 2014; Moffett et al., 2007).

## 2. Data and methods

### 2.1. Study area

Guayaquil is located on the western bank of the Guayas River ( $79^{\circ}50' - 79^{\circ}59' \text{ W}$  and  $2^{\circ}02' - 2^{\circ}18' \text{ S}$ ) and is the capital of the Ecuadorian province of Guayas. It is the largest and the most populous city in Ecuador, with  $1800 \text{ km}^2$  of total area and an estimated population of 2.69 million (Castillo et al., 2011). The climate in Guayaquil is considered to be tropical humid, with a mean annual temperature of  $26^{\circ}\text{C}$  and mean precipitation of 1030 mm. Its proximity to the Pacific Ocean allows cold (Humboldt) and warm (El Niño) currents to mark two distinct weather periods (Johansson et al., 2017). The city has a wet and rainy season (during which 97% of annual precipitation occurs) from January to May, also the season of highest dengue incidence, while the dry season persists from June to December (Castillo et al., 2011; Pourrut, 1983).

Total dengue cases are presented with climate data for Guayaquil during the period 2000–2017 (Fig. 1). Fig. 1a shows fairly high average air temperature and low wind speeds in the city (Johansson et al., 2017). There is a evident seasonal peak in dengue transmission from February to June (dengue season) following the onset of the rainy season (Fig. 1b) along with variation in humidity, water vapor pressure (Fig. 1c), and air temperature (Castillo et al., 2011; Lippi et al., 2018). The influence of climate on dengue is evident one to two months later, since *A. aegypti* requires 7 to 45 days to go from egg to adult (Karim et al., 2012). Currently, DF is considered hyper-endemic in the coastal lowland region of Ecuador where all four serotypes of the disease have been circulating since 2000 (Alava et al., 2005; Real-Cotto et al., 2017;

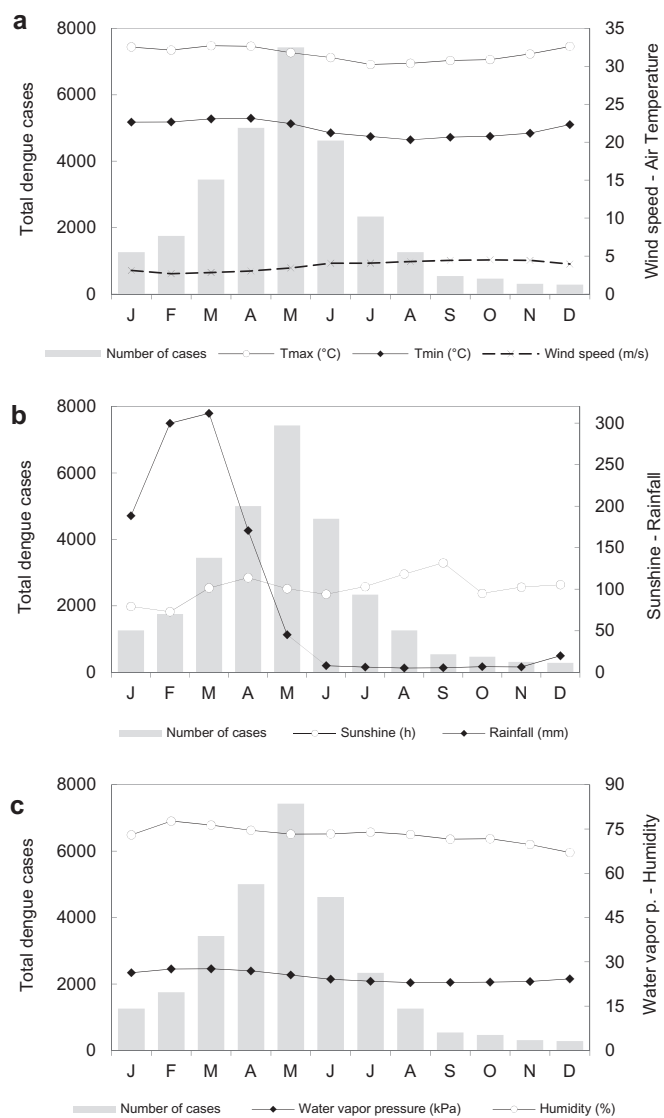


**Fig. 1.** Total dengue cases according to climate in Guayaquil for the period 2000–2017. (a) Mean monthly maximum air temperature (Tmax), minimum air temperature (Tmin), and wind speed. (b) Mean monthly sunshine and rainfall. (c) Mean monthly water vapor pressure and humidity.

Stewart-Ibarra et al., 2013).

Ecuador is divided into administrative territories known as zones, districts and circuits that are designed for providing efficient services (SENPLADES, 2013). Districts are used by the Ministry of Public Health of Ecuador to coordinate health services within the city as well as to organize disease reports and data. In this research, we used districts to represent sectors of Guayaquil that include neighborhoods and parishes (Fig. 2) to better explain our results.

### 2.2. Climatic, epidemiological and social data

Average monthly climatic data for precipitation (mm), solar radiation ( $\text{kJ m}^{-2} \text{ day}^{-1}$ ), water vapor pressure (kPa), wind speed ( $\text{m s}^{-1}$ ), maximum and minimum temperature ( $^{\circ}\text{C}$ ) were obtained from WorldClim version 2. These data represent the period 1970–2000 and are provided as 12 raster files with a spatial resolution of  $1 \text{ km}^2$  or 30 arc-seconds (Fick and Hijmans, 2017).

The National Secretary of Higher Education, Science, Technology and Innovation of Ecuador provided epidemiological and meteorological data for this study. The data sets derive from a collaborative

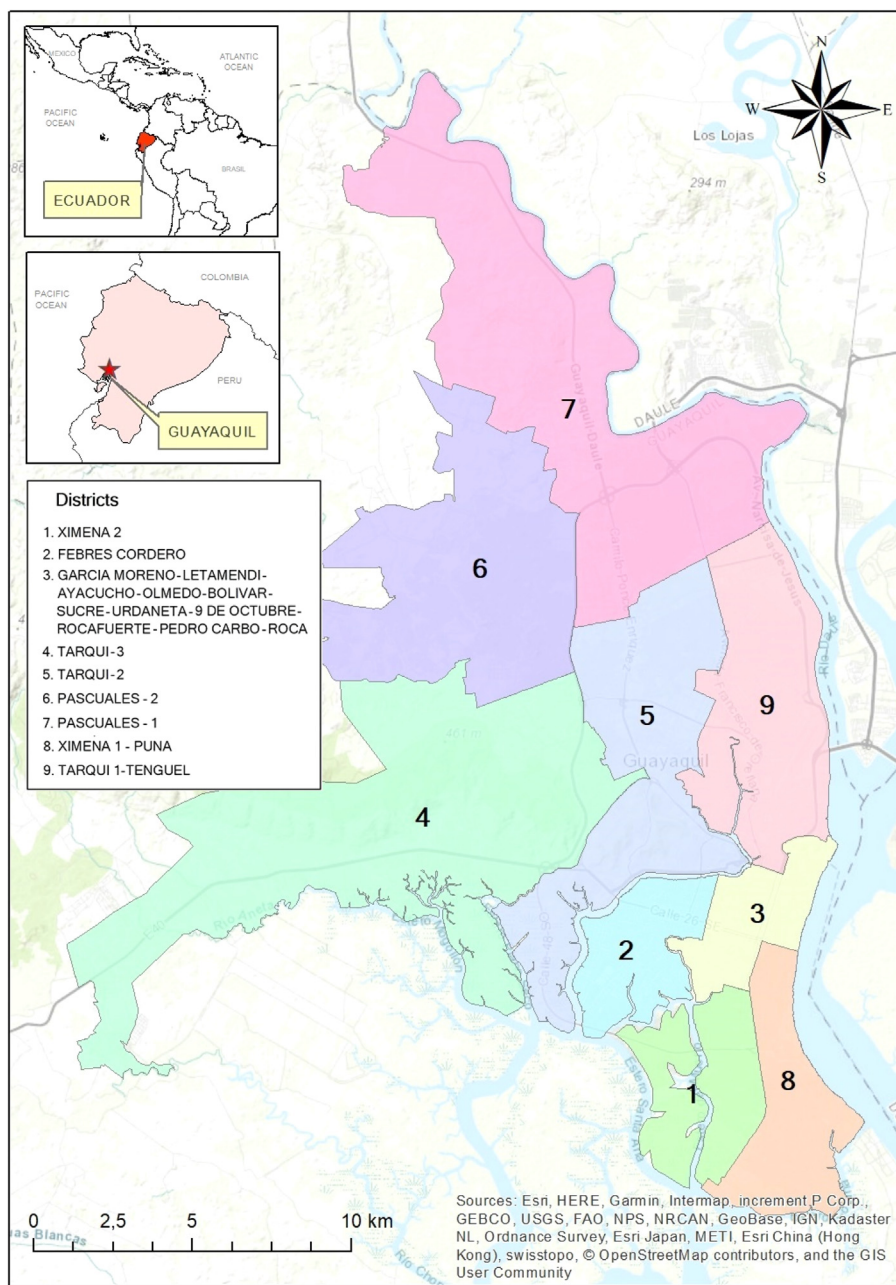


**Fig. 2.** Districts within the urban area of Guayaquil.

project between the National Institute of Meteorology and Hydrology of Ecuador and the Ministry of Health that was sponsored by the Ecuadorian government. The information includes a shapefile of georeferenced dengue cases reported in Guayaquil during 2012, containing a total of 4248 observations, which corresponds to the 15% of total dengue cases confirmed by the Ministry of Health at the national scale in the same year (Ministerio de Salud Pública del Ecuador, 2013). The data were used as presence records and were previously de-identified and organized as census zone polygons to protect individual identities (Hartner et al., 2013; Lippi et al., 2018). Each georeferenced site shows specific records of clinically suspected and confirmed cases of DF and dengue hemorrhagic fever (grouped as total dengue cases) (Lippi et al., 2018). The Moran's I method was applied to the dengue data using ArcMap 10.5 to test whether dengue cases were randomly distributed in space (Stewart-Ibarra et al., 2014). Moran's I is a spatial autocorrelation technique that provides an index of dispersion ranging from  $-1$  to  $1$ , where  $-1$  indicates good negative spatial autocorrelation (dispersed),  $0$

shows perfect spatial randomness, and  $1$  indicates positive spatial autocorrelation (clustered) (Tu and Xia, 2008).

The geographical information also included data from the Ecuadorian National Census of 2010 at the household level, incorporating 24 social variables related to factors such as demography, level of education, municipal services, and socio-economic aspects of Guayaquil (Table 1) (INEC, 2010). The variables included a normalized housing condition index (HCI) created for each household by combining three housing variables as shown in Eq. (1) (Lippi et al., 2018; Stewart-Ibarra et al., 2014).

$$HCI = \frac{[(CR + CW + CF) - \min]}{(\max - \min)} \quad (1)$$

where CR stands for condition of the roof, CW is the condition of the walls, and CF is the condition of the floors. The results are presented in a range from  $0$  to  $1$ , where  $1$  is the worst (Stewart-Ibarra et al., 2014).

**Table 1**  
Descriptive statistics for social and climatic variables.

Variable	Abbreviation	Mean (%)	Skewness	Tolerance	VIF	Std. deviation
<b>Social variables</b>						
Access to paved roads	nopave_per	18.985	1.434	0.257	3.893	0.272
Afro-Ecuadorians	afro_per	10.119	1.921	0.449	2.226	0.087
Head of household has post-secondary education	postsec_pe	25.924	1.031	0.056	17.719	0.223
Head of household has primary education or less	prim_per	30.831	-0.038	0.079	12.734	0.169
Head of household has secondary education	sec_per	31.675	-0.448	0.316	3.164	0.093
Head of household is unemployed	unemploy_p	27.057	0.295	0.370	2.703	0.084
Head of household is a woman	womhead_pe	33.438	-0.114	0.625	1.601	0.064
House conditions	housecond	26.679	-0.119	0.117	8.515	0.135
Mean age of the head of household	headhh_age	45.855	-0.104	0.081	12.373	4.884
Mean household age	hh_age	29.497	0.436	0.039	15.515	4.580
> 4 people per bedroom	fourplbed	16.748	-0.051	0.208	4.815	0.099
Municipal garbage collection	nogarbage	6.126	1.636	0.467	2.142	0.153
Municipal sewage	nosewer_pe	36.604	0.597	0.220	4.540	0.403
Number of households	households	126.385	-0.235	0.068	14.614	6.895
People emigrate for work	emigrant_p	1.908	1.085	0.668	1.497	0.017
People in household drink tap water	drinktap_p	76.853	-0.682	0.358	2.797	0.113
People per household	pplperhh	3.881	1.125	0.483	2.069	0.600
Piped water inside home	nopiped_pe	22.155	1.860	0.173	5.775	0.307
Population inside the household	pop	493.354	0.082	0.051	19.704	5.448
Proportion of household under 15 years of age	under15_pe	28.161	0.101	0.078	12.753	0.071
Proportion of household under 5 years of age	under5_per	9.204	0.676	0.174	5.752	0.031
Receive remittances	remittance	8.919	0.493	0.452	2.212	0.053
Rental homes	rental_per	22.948	0.892	0.319	3.139	0.170
Unoccupied household	unocc_per	16.540	1.793	0.777	1.287	1.839
<b>Climatic variables</b>						
Precipitation (mm)	prec	1086.672	-3.462	0.480	8.653	7.170
Solar radiation ( $\text{kJ m}^{-2} \text{ day}^{-1}$ )	rad	12,974.415	-0.606	0.871	9.448	3.583
Maximum temperature (°C)	tmax	29.665	-2.383	0.847	9.833	0.283
Minimum temperature (°C)	tmin	21.001	-2.316	0.375	8.915	0.711
Water vapor pressure (kPa)	vapr	2.487	-2.540	0.359	6.627	0.084
Wind speed ( $\text{m s}^{-1}$ )	wind	1.832	-3.297	0.792	8.315	0.098

VIF stands for Variance Inflation Factor. Tolerance values < 0.10 and VIF values great than 10 indicate multicollinearity (Dormann et al., 2013; Lomax and Hahs-Vaughn, 2012).

### 2.3. MaxEnt/GIS model

The basic concept of the maximum entropy (MaxEnt) model mentions that the real distribution of a species is represented as a probability distribution over the set of sites in the study area (Phillips and Dudík, 2008). The algorithm is capable to generate a model of probability distribution that uses a set of constraints resulting from the occurrence data which are expressed as functions of the environmental variables, known as features. (Elith et al., 2011; Phillips et al., 2006; Phillips and Dudík, 2008). Since the georeferenced dengue cases reported in Guayaquil during 2012 were used as presence records and absence data were not obtained, we applied the MaxEnt software version 3.4 (Phillips et al., 2017) due to its capacity to analyse presence-only records with decent performance (Elith et al., 2011; Fatima et al., 2016), assuming the vector presence where DF cases were reported and georeferenced. When MaxEnt is applied to presence-only species distribution modeling, the pixels of the study area integrate the space on which the probability distribution is defined (Phillips et al., 2006; Phillips and Dudík, 2008). This model uses a subset of the original data to validate the model, where the dataset is divided into training and testing data in order to generate predictions and assess its accuracy (Elith et al., 2006; West et al., 2016). Therefore, it is stated that if testing data are satisfactorily predicted properly by the model, then the model is considered to accurately predict the species' range (Moya et al., 2017; West et al., 2016).

In this study, we derived a potential spatial distribution model of DF at the city scale using MaxEnt to test the hypothesis that social-ecological variables were associated with the presence of the disease in Guayaquil, Ecuador during 2012, considering that social and environmental conditions favour the extensive distribution of the vector causing high epidemiological risks (Cardoso-Leite et al., 2014; Lippi

et al., 2018). The data were prepared using ArcMap 10.5 and the same coordinate system (GCS\_WGS\_1984) was assigned to the files for each variable. All layers were cut according to the study area using the 'extract by mask' tool, verifying that the 'processing extent' is the same for each variable within 'environment settings' in order to ensure that all files cover exactly the same area (Ifaei et al., 2017; Jácome et al., 2018). The 'resample' tool was used to guarantee the same spatial resolution (cell size X 0.0001, Y 0.0001) for all raster files. MaxEnt software requires ASCII (.asc) format for input, and therefore, 'convert raster to ASCII' was used to reformat each file. To assess model performance, we defined 25% presence as indicating random test data and 75% presence was selected for training using a logistic output format. The 'random seed' selection was used to guarantee that the model chooses different sets of presence records for training and testing on every replicate (Fatima et al., 2016; Moya et al., 2017). Additional settings (convergence threshold: 0.001, maximum number of background points: 10000, maximum iteration: 5000, auto features) were kept as default. The final maps were generated using ArcMap 10.5.

Model performance was evaluated using the area under the curve (AUC) of the receiver operating characteristic curve (ROC). This is a plot of sensitivity versus 1-specificity and measures the ability of the MaxEnt model to discriminate between presence and background sites (Phillips and Dudík 2008; Pavez-Fox and Estay, 2016; Moya et al., 2017). In this approach, 'sensitivity' refers to the fraction of observed presences predicted by the model, quantifying omission errors, and 'specificity' is the fraction of observed absences predicted as such, quantifying commission errors (Cardoso-Leite et al., 2014). The AUC values were evaluated based on predictive precision according to the following criteria: excellent (1–0.9), good (0.9–0.8), acceptable (0.8–0.7), bad (0.7–0.6), and invalid (0.6 – < 0.5) (Araujo et al., 2005). Variable importance was analyzed using the jackknife test in order to

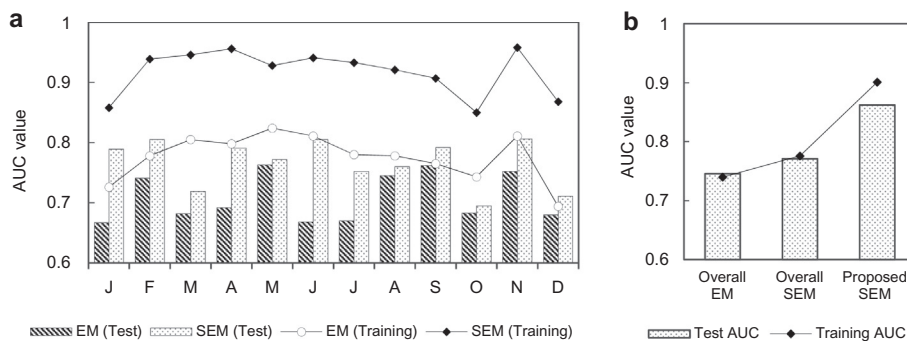


**Fig. 3.** Area under the curve (AUC) values of receiver operating characteristic curves (ROC) for performance evaluation based on training and test datasets. (a) Results of ecological models (EM) and social-ecological models (SEM) of each month of 2012. (b) Results of overall EM, overall SEM and the proposed SEM using UBN components.

identify the most effective single variable for predicting distribution. This test shows the ‘gain’ of each predictor variable, which is an indication of how much better-than-random the model fit is. A high gain of a specific variable indicates greater predictive value (Phillips et al., 2017). Descriptive statistics were obtained using Matlab.

One EM and one SEM were implemented to explore the influence of social variables on model accuracy and also to identify the most important variables determining the dynamics and ecology of *A. aegypti* in Guayaquil. In the EMs, climatic variables were included by using files corresponding to each month of the year, therefore obtaining 12 different models. The same process was used for the SEMs, but this time 24 social variables with fixed values derived from the Ecuadorian National Census of 2010 at the household level as previously described were added to the models for each month. Such analysis allows us to evaluate the variability of the probability of occurrence of dengue throughout the year. The ‘raster calculator’ of ArcMap software was used to convert the monthly climatic files into a single annual file in order to perform an overall EM and an overall SEM.

Once the overall SEM was generated and variables with the greatest influence on model performance were identified, we grouped social factors based on the concept of unsatisfied basic needs (UBN) (Feres and Mancero, 2001) and created new indexes to summarize their basic characteristics and patterns in order to obtain more reliable accuracy for the MaxEnt model. According to the Economic Commission for Latin America, social factors considered in the analysis of UBN must determine a set of needs that must be met by a household so that their standard of living is considered worthy, according to the standards of the society to which it belongs. Basically, it refers to a set of conditions that a home must have to be considered to be “not poor” (Friz and Fernandez, 2015; Feres and Mancero, 2001; SENPLADES, 2013).

#### 2.4. Prediction of cases with partial least squares regression

Additional climate and epidemiological data was shared by the National Secretary of Higher Education, Science, Technology and Innovation and the Ministry of Health of Ecuador in the form of a time series data set of monthly meteorological values for 8 variables (rainfall (mm), humidity (%), sunshine (hours), water vapor pressure (kPa), wind speed ( $m s^{-1}$ ), cloudiness (octa), and maximum and minimum temperature ( $^{\circ}C$ )) of the period 2000–2012, measured by the weather station of Universidad Estatal de Guayaquil ( $2^{\circ}12'0'' S$ ,  $79^{\circ}53'0'' W$ ) and operated by the National Institute of Meteorology and Hydrology of Ecuador. Dengue cases reported per epidemiological week in Guayaquil during 2000–2017 were also obtained. These cases were based on clinical diagnosis rather than laboratory confirmation due to the low rate of laboratory confirmation. All data were used together to derive a predictive model of DF including a future forecast for the year 2020.

Partial least squares regression (PLS-R) was used in a temporal analysis to predict dengue cases using climatic data and identify the most important meteorological factors influencing the disease in Guayaquil using variable importance in the projection (VIP) analysis

where variables with values greater than one are considered to be ‘important’ (Islam, 2012; Akarachantachote et al., 2014). The model included a future dengue forecast using the predictive equation generated by PLS-R and an autoregressive model in order to estimate future climatic conditions. Variables that were not normally distributed were log-transformed and the data set was centered and standardized, since all variables were not measured with the same units (Li et al., 2002). The model was implemented with a monthly time lag and high outliers were reduced to obtain better estimates. SIMCA software was used to perform the analysis and a permutation validity testing with the aim of comparing the  $R^2$  and  $Q^2$  of original data with the goodness of fit of several Y-random permuted models, with the X-matrix kept intact (Islam, 2012; Touhami et al., 2016). Additional spatially-predicted climatic data for the year 2020 was obtained from the GIS Climate Change Scenarios website ([gisclimatechange.ucar.edu/gis-data](http://gisclimatechange.ucar.edu/gis-data)) using the A2 climate change scenario, since it is considered to be the more realistic currently (Cardoso-Leite et al., 2014; IPCC, 2007). A2 scenario can be considered as a description of the world’s evolution in case of maintaining our current behavior. It describes a heterogeneous world with a continuous growth of population, an economic development oriented basically to the regions, and independently operating self-reliant nations (IPCC, 2007).

## 3. Results

### 3.1. Model performance

Records of the presence of DF at the household level for 2012 showed cases to be significantly clustered (Moran’s  $I = 0.663$ ;  $p$ -value < .05) with < 1% likelihood that this clustered pattern could be the outcome of random chance. We considered six climatic variables and 24 social variables for the MaxEnt models, where 7 of the 30 tested variables had VIF scores above 10 (Table 1). Our performance evaluation showed that SEMs performed better than EMs for tests and training (Fig. 3a). The monthly EM of 2012 obtained ‘good’ performance with training AUC values between 0.72 and 0.81. The monthly SEMs showed training AUC values between 0.85 and 0.96, considered to indicate ‘very good/excellent’ performance.

The EM output suggests that January, March, April, June, and December are months with the greatest probability of occurrence (values > 0.8), of which April has the highest value (0.974) (Fig. A1). This prediction agrees with actual records for the dengue outbreak of 2012 that occurred during the wet season. Therefore, the probability of disease decreases spatially during the dry season. Jackknife tests of the models indicate that the contribution of precipitation is variable throughout the year. Maximum air temperature (Tmax) and minimum air temperature (Tmin) have high contributions when high suitability is observed, together with water vapor pressure that also exhibited high contribution for seven months. Solar radiation and wind speed increased in influence during months when outbreaks occurred.

However, SEMs showed greater accuracy in terms of probability

values, as well as in spatial visualization of the sites of greatest concern since the social variables included described data at the household level. The output of SEMs shows probabilities of occurrence higher than 0.9 for all months, which indicates better performance (Fig. A2). The spatial distribution increases gradually from February and remains stable until August, with its biggest peaks during April and May. The probability decreases spatially from September to December. These results indicate that the southern and south-central districts, including Tarqui 1, Tarqui 2 and the southern portion of Pascuales 1, are places with the greatest risk of DF infections. Low contributions of social variables are observed in months during which greater areas exhibit low probabilities of infection (September to December, including January). Significant influences of social variables are observed during DF season, especially those variables related to population density, access to piped water, and level of education of head of household. However, ‘unemployment’ exhibited high contributions throughout the year, most likely since it is associated with low incomes and poverty. Similar results are observed for ‘unoccupied households’ since the vector mosquito can easily find stagnant water in such places, where it can persist for longer periods of time.

Our model performance assessment also showed that the overall EM yielded poorer training performance (training AUC = 0.740) compared with the overall SEM (training AUC = 0.776) and similar results for testing data. Therefore, the results of SEM are considered more reliable. The maps for the overall models and jackknife tests are shown in Fig. 4. Considering a threshold of 0.05 in the regularized training gain of the jackknife test for the overall SEM, all six climatic variables and 12 social variables were found to be important for this model: head of household has post-secondary education, head of household has primary education or less, head of household has secondary education, head of household is unemployed, head of household is a woman, house conditions, > 4 people per bedroom, municipal garbage collection, people in household drink tap water, piped water inside home, population inside the household, unoccupied household. Therefore, these social factors are associated with the presence and burden of DF in Guayaquil which also played important roles in the 2012 outbreak.

### 3.2. Social-ecological model based on UBN and climatic data

Since the overall models resulted in very low accuracy and the method we used to generate overall models is the method most commonly used for generating maps of potential disease distribution, we proposed using groups of the most important variables previously identified to improve the performance of the overall SEM, an amendment that also eliminates collinearity between certain variables. It was determined that most of the social factors match with components of UBN as established by the Economic Commission for Latin America (Fig. 5). Therefore, new variables were created based on the corresponding UBN components, to which weights were assigned according to their importance as shown in eqs. 2–4.

$$BHS = [(0.4Pw) + (0.4Gc) + (0.2Tw)] \quad (2)$$

$$LE = [(0.5Pe) + (0.3Se) + (0.2Pse)] \quad (3)$$

$$EC = [(0.5Un) + (0.5Pop)] \quad (4)$$

where, *BHS* stands for access to basic housing services; *Pw*: piped water inside home; *Gc*: municipal garbage collection; and *Tw*: people in household drink tap water; *LE*: level of education; *Pe*: head of household has primary education or less; *Se*: head of household has secondary education; *Pse*: head of household has post-secondary education; *EC*: economic capacity; *Un*: head of household is unemployed; *Pop*: population inside the household.

The new model was applied using the six climatic variables along with basic housing services, level of education, economic capacity, house conditions, and overcrowding which corresponds to the variable

‘more than 4 people per bedroom’. Additionally, ‘head of household is a woman’ and ‘unoccupied household’ were included since they were in the original group of the 12 most important social variables. The performance of our proposed model using UBN components showed better accuracy than the other models, obtaining a higher AUC value (excellent) compared with previous overall models (Fig. 3b).

### 3.3. Spatial dynamics

The final map of potential spatial distribution of DF in Guayaquil based on SEM performed with UBN shows that the areas with the highest risks of infection (probability of occurrence between 0.7 and 0.9) are mainly located in the south of the city, covering an area of approximately 50.81 km<sup>2</sup> (Fig. 6a). Febres Cordero shows uniform high probability across the entire territory, as does the northwest of Ximena 2. Ximena 1 obtained the highest suitability for DF occurrence from its center to the southern end, while within district 3 (which groups several urban parishes together) the maximum probability is observed in the south part decreasing progressively toward the north. Our findings suggest that these areas must take priority when integrated vector-control interventions are performed. The central section of the city shows a more optimistic situation due to low probability of infections, a finding that extends along Tarqui 3 and the southern portions of Tarqui 1 and Tarqui 2. In the northern portions, we observed a pattern of spatial distribution that concentrates high probability toward the center of this part of the city. This pattern corresponds with areas of higher population density in Pascuales 1, Pascuales 2 and Tarqui 2. All these sectors are characterized by low socio-economic living standards and limited access to public utilities (Castillo et al., 2011).

Jackknife tests of the proposed model indicate that precipitation, solar radiation, and Tmax contribute the most influence on the spatial distribution model and can be considered the most important meteorological factors influencing dengue spread in Guayaquil (Fig. 6b). The most important social risk factors associated with the presence of cases of DF were ‘head of household is a woman’ and ‘unoccupied household’, including poor structural conditions of floors, roofs, and walls, as well as access to municipal basic housing services and overcrowding at the household level. Another factor positively associated with the number of dengue cases was the proportion of heads of household with low levels of education.

The response curves of one-variable-models created using only the corresponding variable represent the probability of dengue occurrence according to each variable (Fig. 6c). The first curve demonstrates that habitat suitability decreases as the index of access to basic housing services and level of education of the head of the household increases. In terms of structural quality of houses, the response curve indicates that disease probability increases as house conditions worsen. The remaining variables show positive correlations between suitability and the growth of their conditions. The response curve to precipitation specifies 1000 mm and 1150 mm as ideal rain fall conditions for the expansion of the disease in Guayaquil. The influence of solar radiation is variable; however, the curve establishes 15,000 kJ m<sup>-2</sup> day<sup>-1</sup> as a maximum value. There is high probability when Tmax reaches between 29.5 °C and 30.1 °C and Tmin ranges between 20.6 °C and 21.2 °C. Additionally, 2.52 kPa was determined as a maximum value for water vapor pressure and 1.8 m s<sup>-1</sup> for wind speed, as higher values decrease habitat suitability and therefore the conditions for the transmitter vector become less favorable.

### 3.4. Predictions of numbers of cases and future forecasts

VIF results eliminated the possibility of collinearity issues since all climatic variables used for this analysis had VIF scores of < 10 and tolerance values greater than 0.10 (Table 2). The results of analyses including two latent variables accounted for 78.5% of the variability of the Y-variable (*R*<sup>2</sup> = 0.785 and *Q*<sup>2</sup> = 0.573). Similar *R*<sup>2</sup> values were

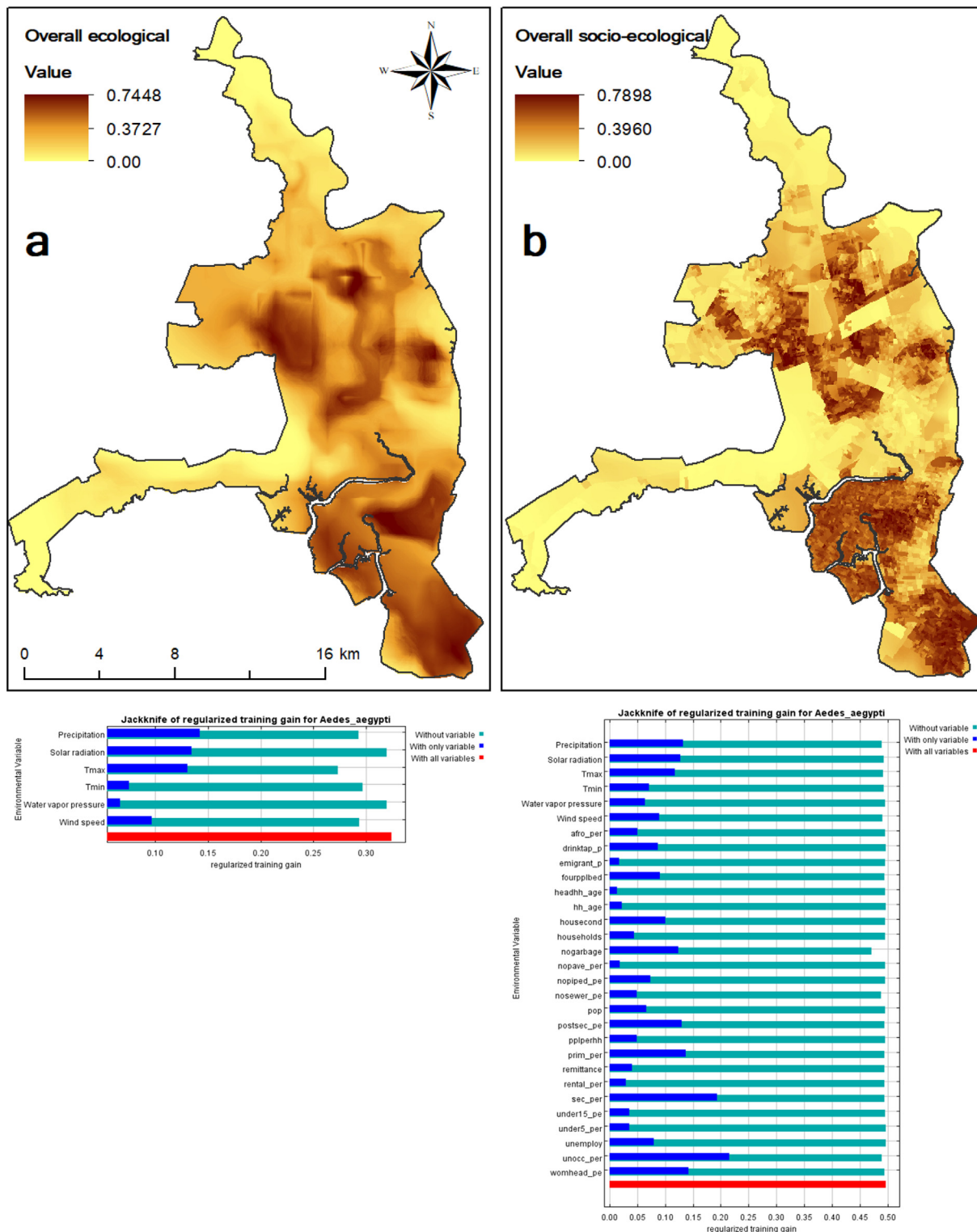


**Fig. 4.** Results for the (a) overall ecological model (EM) and (b) overall social-ecological model (SEM). Each map includes jackknife test results.

obtained in previous studies that also applied regression methods (Islam, 2012; Karim et al., 2012; Lee et al., 2016). Our model was determined to be valid due to fulfillment of the evaluation criteria of the permutation validity test. VIP analysis identified Tmin, Tmax, humidity, and cloudiness as the most important variables in the projection (Table 2), which exert the greatest influence on DF in Guayaquil since 2000. The PLS-R equation was used to predict total dengue cases and its coefficients shows that all variables are significant.

The comparison curve of observed and predicted values shows that the predicted values mirror intra-seasonal variability in the number of dengue cases in Guayaquil during 2000 and 2017, although the model predicted slightly lower numbers of dengue cases than were observed during high outbreaks, a finding that is most evident for the 2015 outbreak. The observed and predicted total dengue cases values showed significant correlation, since the Spearman correlation coefficient obtained values  $> 0.721$  ( $p < .05$ ). The regression plot of the Y-variable

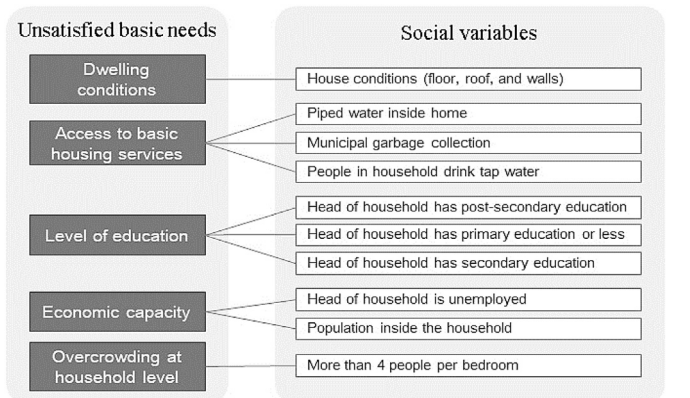


**Fig. 5.** Social factors fitting within the components of unsatisfied basic needs (UBN) established by the Economic Commission for Latin America.

(observed vs. predicted) resulted in  $R^2 = 0.865$ . It was also determined that dengue outbreak seasons starts in February and ends between June and July, with the highest incidence during March and April of each year, corresponding to the highest average temperatures of the wet seasons during the study period. The incidence forecast for 2020 suggests that outbreaks will follow the trends observed since 2010 (Fig. 7). However, the worst outbreak is estimated to occur in 2018.

The map of the potential spatial distribution of DF in Guayaquil for

**Table 2**  
PLS-R coefficients and variable importance in the projection (VIP) analysis.

Variable	VIP	Coefficient	Mean	Tolerance	VIF
Intercept	–	–11.510	–	–	–
Tmin (°C)	1.541	3.902	21.466	0.402	2.486
Tmax (°C)	1.201	–4.386	31.724	0.389	2.572
Humidity (%)	1.107	4.756	72.786	0.324	3.088
Cloudiness (octa)	1.087	2.438	5.932	0.403	2.479
Water vapor pressure (kPa)	0.913	3.285	24.868	0.187	5.339
Rain fall (mm)	0.824	0.091	89.130	0.341	2.929
Sunshine (hours)	0.450	–0.463	101.483	0.856	1.168
Wind speed ( $m s^{-1}$ )	0.243	–0.243	3.767	0.715	1.399

the year 2020 that was derived using predicted climatic data from the A2 climate change scenario shows that the coverage area of highest probability (0.7–0.9) will increase from  $50.81 \text{ km}^2$  as observed in 2012, to  $80.75 \text{ km}^2$  during 2020, increasing the area of high infection risk in the north-central and southern portions of the city (Fig. 8). Our results indicate that the incidence of DF in 2012 and 2020 should be similar, but the spatial analysis demonstrates that the potential spatial distribution of the disease during 2020 is larger.

#### 4. Discussion

Year 2012 had a high incidence of DF with intense endemic-epidemic transmission and variability in behavior (Real-Cotto, 2017). All

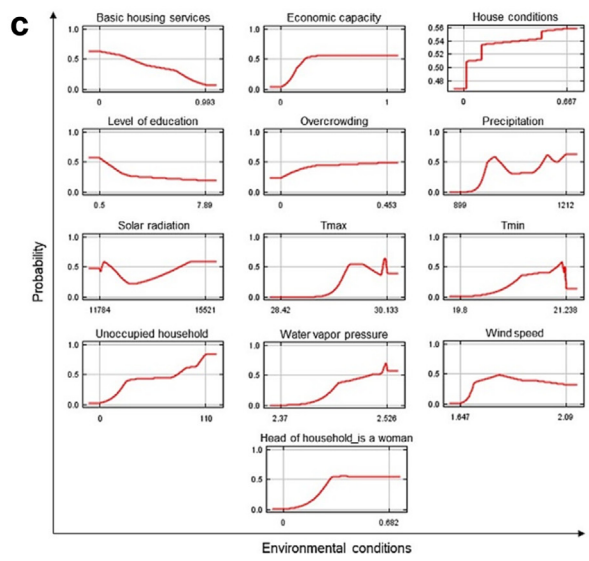
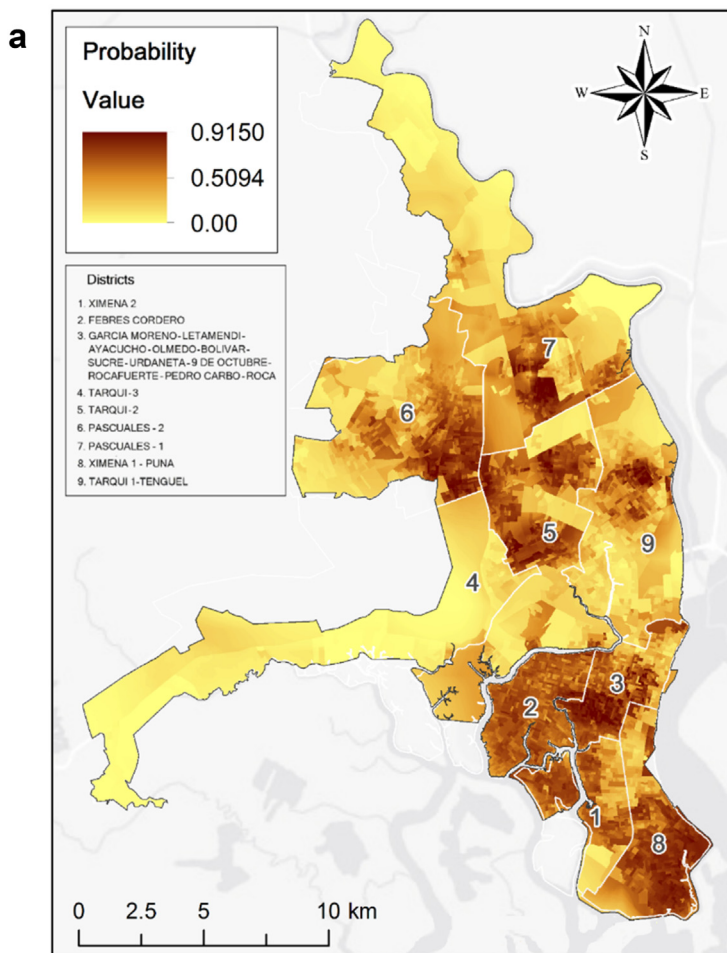


**Fig. 6.** (a) Final map of potential spatial distribution of dengue fever in Guayaquil based on the proposed SEM model performed with unsatisfied basic needs (UBN). (b) Jackknife test. (c) Response curves of one-variable-models.

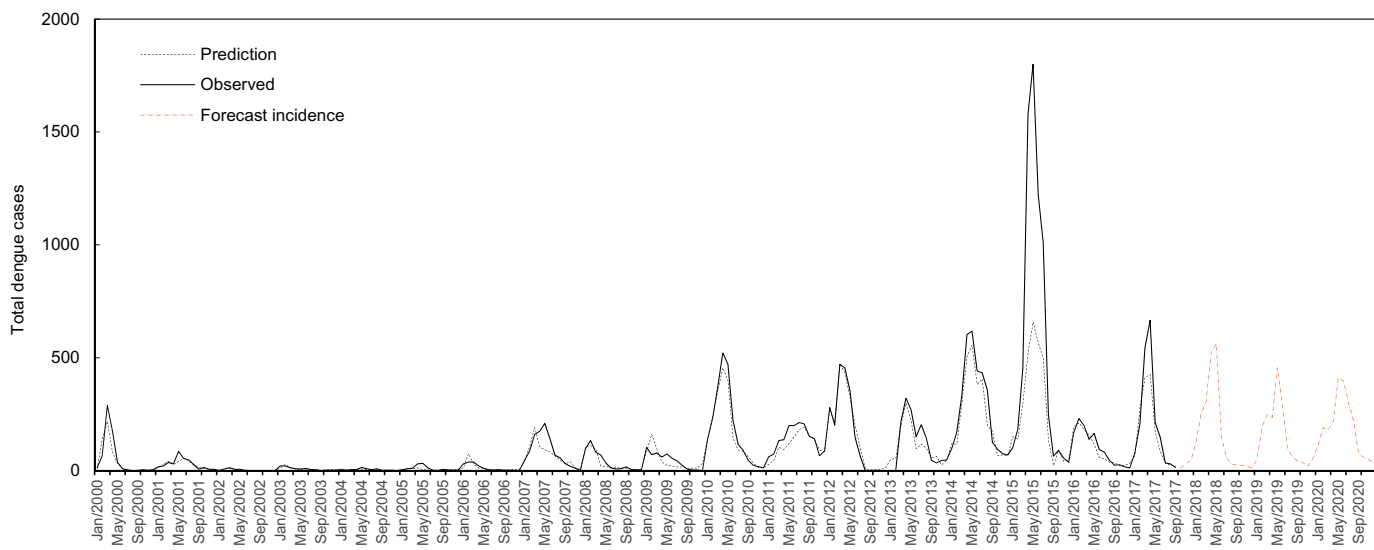


**Fig. 7.** Prediction of total dengue cases during 2000 and 2017 using monthly climatic data and a forecast of dengue incidence for 2020.

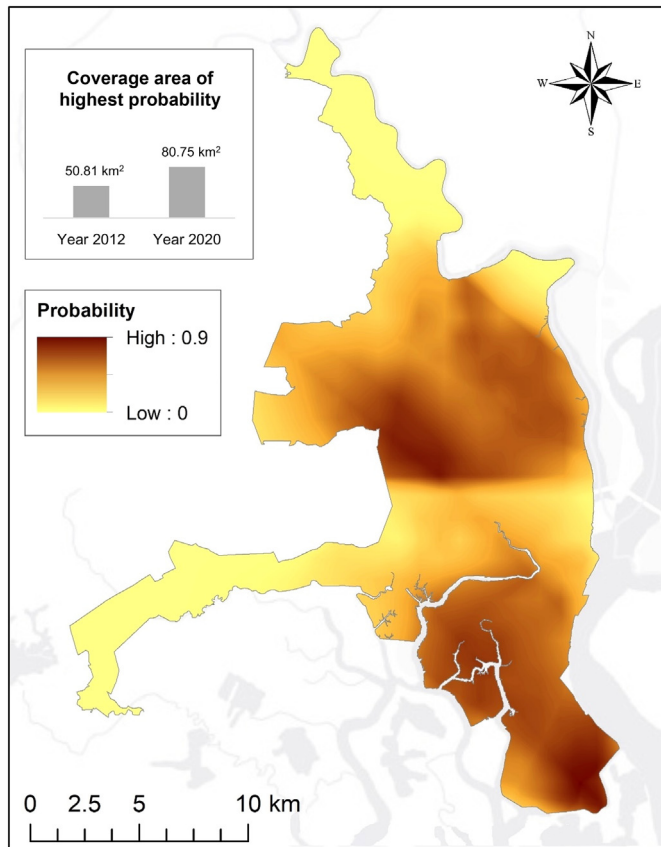


**Fig. 8.** Map of potential spatial distribution of dengue fever in Guayaquil for the year 2020 based on predicted climatic data for the A2 climate change scenario, with the coverage area of highest probability of occurrence.

four serotypes of dengue virus are present in Guayaquil, with simultaneous circulation of three of them, which has created a situation where residents are at high risk of severe dengue in the near future, based on the events of previous decades in Guayaquil and neighboring countries (Real-Cotto, 2017; Real-Cotto et al., 2017). According to a cluster analysis performed by Castillo et al. (2011) using spatial distributed data for DF during the period 2005–2009, the grouping patterns of DF cases varied each year. From 2005 to 2007, the main clusters were

observed in the northwest portion of the city and a smaller but significant cluster was observed in the southwest. During 2008 and 2009, the cluster in the north was considerably reduced and new important concentrations of cases appeared in the southernmost region (Castillo et al., 2011).

In the neighborhoods where greatest risk of dengue infection has been identified, vector control activities focus on the application of larvicidal products provided by public health workers, although homeowners tend not to use directly distributed larvicides (Lippi et al., 2018). Therefore, human behavior and socio-economic factors are strongly connected to the spatial transmission dynamics of DF, a finding that agrees with those of several previous studies (Gubler, 2002; Mondini and Chiaravalloti, 2008; Reiter et al., 2003; Zhu and Lin, 2018). Our results constitute evidence that the main cluster patterns of DF identified by Castillo et al. (2011) in the northwest, southwest, and southern portion of the city during the period 2005–2009, were concentrated in 2012. However, it is clear that the areas of risk were considerably extended toward the east and the north due to the high incidence of disease during 2012, which could have been influenced by the strong climatic conditions of El Niño Southern Oscillation (Real-Cotto, 2017).

It is important to mention that the household level data used in this study does not encompass the quality of services. However, it is well known that water supply interruptions or frequency of garbage collection have direct influence on mosquito breeding sites (Lippi et al., 2018), which demonstrates that good access to municipal services can reduce the amount of larval habitat (Mulligan et al., 2015), but it is also important to consider that significantly populated and urbanized neighborhoods offer plenty habitat regardless of services accessibility (Mulligan et al., 2015; Teurlai et al., 2015). Stewart-Ibarra et al. (2013) documented positive correlations between DF infections and deficient services as the lack of sanitation and water supply in Machala, Ecuador, and identified these as problems that generate habitats for larval mosquitoes. All these factors are related to poverty and although the relationship between poverty and DF transmission has not been well established, the association between poor housing conditions and dengue infections has been well studied by researchers around the world (Koch et al., 2016; Lippi et al., 2018; Mulligan et al., 2015; Van Benthem et al., 2005).

Education was another important factor identified in our study since levels of education and knowledge of population regarding prevention practices and elimination of mosquito breeding sites are essential for disease control activities (Teurlai et al., 2015). Therefore, to maximize

the success of future prevention campaigns it is necessary to alter negative attitudes that local populations may have regarding to prevention practices (Alyousefi et al., 2016), but we must also consider that perceptions of DF differ between urban sectors according to social and economic features (Stewart-Ibarra et al., 2014). According to the World Health Organization, the overall objectives of public health surveillance that are applicable to DF are related to the early recognition of epidemics for appropriate intervention, measures of disease burden, monitoring trends in the distribution and spread of disease over time and space, the monitoring of environmental risk factors, and the efficacy of prevention and control programs (Gubler, 2002; WHO, 2012). The prevention of dengue infections depends on interrupting human–vector contact by controlling mosquito habitats and the presence of all four mosquito life stages inside households and in household vicinities. These goals can be accomplished through a combination of environmental management, chemical control, and biological control (Ministerio de Salud de la Nación, 2013; Wen et al., 2006). Habitats are eliminated by emptying and cleaning containers as well as by using insecticides, biological agents, and applying adulticides (Ministerio de Salud de la Nación, 2013). Household insecticide aerosol products, mosquito coils, or other insecticide vaporizers can decrease indoor biting activity. Household fixtures such as door and window screens and air-conditioning can also reduce biting (WHO, 2009, 2012). Hence, it is important to mention that the results of our study are suggestive for vector control intervention and follow the same trend of previous studies that use field information and focus on the processes within DF cycle in Guayaquil (Lippi et al., 2018; Real-Cotto, 2017; Real-Cotto et al., 2016).

The framework for building distribution models of DF used in this study is an effective approach for exploratory studies looking to analyse a large number of social-ecological patterns and dynamics. The approach also allows researchers to test multiple hypotheses simultaneously and detect important variables. Our proposed model has demonstrated that performance can be improved by grouping social factors in UBN which can also eliminate collinearity issues. Statistical methods are widely applied to eliminate multicollinearity in species distribution models which ensure a mathematical validation (Cardoso-Leite et al., 2014; Dormann et al., 2013; Fatima et al., 2016; Moya et al., 2017), although there is a risk of excluding variables and information that could be important for the ecological niche under analysis. Therefore, our results have shown that grouping variables with similar information and assign weights according to their importance generates new variables representing the social reality accurately, leading into a satisfactory MaxEnt model performance. Our efforts could be extended by including detailed data for several years, to allow the evaluation of dengue infections at the beginning of outbreaks in order to observe whether epidemics are more likely to start in neighborhoods with similar features, and whether there are persistent hot spots that produce outbreaks and can therefore be targeted for interventions (Lippi et al., 2018; Stewart-Ibarra et al., 2014; Wen et al., 2006). Field work in order to determine breeding sites and houses infested with the vector's larvae and georeferenced dengue cases would help to improve this model and expose the underlying scenario comprehensively.

In addition to the understanding of the reported relationship between climatic conditions, social factors and dengue cases, it is essential to comprehend the role of land-use and land-cover types to vector breeding ability (Fatima et al., 2016; Montagner et al., 2018; Sarfraz et al., 2012) since previous studies have emphasized that they can be an important risk determinant for dengue infections (Sarfraz et al., 2012; Van Benthem et al., 2005; Vanwambeke et al., 2006). However, it has been reported that connection between land-cover and habitat is not always straightforward and is influenced by landscape features (Cheong et al., 2014; Vanwambeke et al., 2007). For this reason, linking land-cover with mosquito habitat preferences is facilitated greatly by knowledge of mosquito ecology (Montagner et al., 2018; Vanwambeke et al., 2007). Our study could not include land-cover factors due to a

lack of data and would be worth including in a more detailed research in order to perform a detailed review of surrounding landscape and its potential relationship with the dynamics of vector population (Sarfraz et al., 2012).

In the temporal analysis, we observed significant differences between Tmin, Tmax, humidity, and rainfall during the wet seasons that remained similar for each year although the number of DF cases differed. Seasonal dengue incidence during a particular period was associated with climatic factors within the same year, but not with the same months of different years. This demonstrates that additional factors contribute to DF incidence, which influence infection rates at the city scale in co-occurrence with climatic variables. Our results also model progressive temporal growth of DF in Guayaquil expected to be maintained in a sustained manner, reflecting moderate endemic-epidemic transmission from the epidemiological perspective as previously noted by Real-Cotto (2017). Our findings underscore the importance of taking action as soon as possible in order to control DF spread since the spatial analysis of forecast incidence for 2020 reveals a very likely disease scattering throughout the city. Considering that climate change trends for precipitation, temperature and other environmental factors can influence the length of the mosquito immature stages by providing required conditions to the larval habitats (Mweya et al., 2016). In conclusion, our study highlights the necessity and importance of better prevention and control strategies in Guayaquil since a high dengue incidence can also seriously affect the local economy (Bujang et al., 2017; Meltzer et al., 1998).

## 5. Conclusion

We modeled the spatial distribution of DF at the city scale in Guayaquil, Ecuador by including social variables, monthly climatic conditions, and dengue cases reported during 2012. The highest probability of dengue occurrence occurs from January to June which agrees with data from the 2012 outbreak and the timing of the yearly wet season. Social variables showed greater contributions during the same period, which demonstrates their importance in the presence and spread of the disease. The results of our overall models were more accurate when human behavior, societal characteristics, and housing conditions were considered individually, but the best performance was obtained when the most important social variables were grouped as components of the population's UBN.

The most significant social factors were 'head of household is a woman' and 'unoccupied household,' included in the UBN component related to housing conditions, access to municipal basic services, and overcrowding at household level. These suggests that such social aspects played pivotal roles during the 2012 epidemic. Our findings highlight the importance of combining spatial and social-ecological data with georeferenced epidemiological records for the implementation of more efficient surveillance systems. Using this city-scale model, we also determined that temperature is influential upon dengue presence across time and space, with higher probabilities of DF presence when Tmax increases to 29.5 °C - 30.1 °C and Tmin ranges from 20.6 °C - 21.2 °C. Precipitation and solar radiation were also determined to be influential factors. The response curve to precipitation specifies 1000 mm and 1150 mm as ideal rain fall conditions for DF spread. Our models established 15,000 kJ m<sup>-2</sup> day<sup>-1</sup> as a maximum value for solar radiation. Higher values decrease the suitability of mosquito habitat, and therefore the conditions for the transmitter vector become less favorable. Our final map determined the potential spatial distribution of DF infections and identified areas with suitable habitat for the transmitter vector. The districts at the highest risk of infection are located mainly in the north central and southern portions of the city (Pascuales 1, Pascuales 2, Tarqui 2, Febres Cordero, Ximena 1, Ximena 2), which suggests that these areas must take priority in the implementation of vector-control interventions and monitoring for potential future epidemics.

## Acknowledgements

This work was supported by the National Research Foundation of Korea (NRF) grant funded by the Korean government (MSIT) (No. 2017R1E1A1A03070713) and by Korea Ministry of Environment(MOE) as Graduate School specialized in Climate Change. The authors would like to express their gratitude to the National Secretary of Higher Education, Science, Technology and Innovation of Ecuador, the National Institute of Meteorology and Hydrology of Ecuador, the Ministry of Health of Ecuador for the climatic and reported dengue case data used in this study, and to Dr. Anna M. Stewart Ibarra from State University of New York Upstate Medical University for the information and data shared.

## References

Akarachantachote, N., Chadcham, S., Saithanu, K., 2014. Cutoff threshold of variable importance in projection for variable selection. *Int. J. Pure Appl. Math.* 94 (3), 307–322. <https://doi.org/10.12732/ijpm.v94i3.2>.

Alava, A., Mosquera, C., Mosquera, C.E., Vargas, W., Real, J., 2005. Dengue en el Ecuador 1989–2002. *Rev. Ecuator. Higiene y Med. Trop.* 42, 11–29.

Alyousefi, T.A.A., Abdul-Ghani, R., Mahdy, M.A.K., Al-Eryani, S.M.A., Al-Mekhlafi, A.M., Raja, Y.A., Shah, S.A., Beier, J.C., 2016. A household-based survey of knowledge, attitudes and practices towards dengue fever among local urban communities in Taiz Governorate, Yemen. *BMC Infect. Dis.* 16, 543. <https://doi.org/10.1186/s12879-016-1895-2>.

Araujo, M.B., Pearson, R.G., Thuiller, W., Erhard, M., 2005. Validation of species-climate impact models under climate change. *Glob. Chang. Biol.* 11, 1504–1513.

Bujang, M.A., Mudin, R.N., Haniff, J., et al., 2017. Trend of dengue infection in malaysia and the forecast up until year 2040. *Intern. Med. J.* 24 (6), 438–441.

Cardoso-Leite, R., Vilarinho, A.C., Novaes, M.C., Vilardi, G.C., Guillermo-Ferreira, R., 2014. Recent and future environmental suitability to dengue fever in Brazil using species distribution model. *Trans. R. Soc. Trop. Med. Hyg.* 108, 99–104. <https://doi.org/10.1093/trstmh/trt115>.

Castillo, K.C., Körbl, B., Stewart, A., Gonzalez, J.F., 2011. Application of spatial analysis to the examination of dengue fever in Guayaquil, Ecuador. *Procedia Environ. Sci.* 7, 188–193.

Cheong, Y.L., Leitão, P.J., Lakes, T., 2014. Assessment of land use factors associated with dengue cases in Malaysia using boosted regression trees. *SpatialSpatio-Temp. Epidemiol.* 10, 75–84. <https://doi.org/10.1016/j.sste.2014.05.002>.

Dormann, C.F., Elith, J., Bacher, S., Buchmann, C., Carl, G., Carré, G., ... Lautenbach, S., 2013. Collinearity: a review of methods to deal with it and a simulation study evaluating their performance. *Ecography* 36 (1), 027–046. <https://doi.org/10.1111/j.1600-0587.2012.07348.x>.

Elith, J., Graham, C.H., Anderson, R.P., Dudík, M., Ferrier, S., Guisan, A., et al., 2006. Novel methods improve prediction of species' distributions from occurrence data. *Ecography* 29, 129–151.

Elith, J., Phillips, S.J., Hastie, T., Dudík, M., Chee, Y.E., Yates, C.J., 2011. A statistical explanation of MaxEnt for ecologists. *Divers. Distrib.* 17, 43–57. <https://doi.org/10.1111/j.1472-4642.2010.00725.x>.

Eriz, M., Fernandez, M., 2015. Una alternativa para el cálculo de las necesidades básicas insatisfechas (NBI). *Análisis Econ.* XXX (73), 111–138.

Fatima, S.H., Atif, S., Rasheed, S.B., Zaidi, F., Hussain, E., 2016. Species distribution modelling of *Aedes aegypti* in two dengue-endemic regions of Pakistan. *Tropical Med. Int. Health* 21, 427–436. <https://doi.org/10.1111/tmi.12664>.

Feres, J.C., Mancero, X., 2001. El método de las necesidades básicas insatisfechas (NBI) y sus aplicaciones en América Latina. CEPAL, Santiago de Chile (ISBN 92-1-321791-9).

Fick, S.E., Hijmans, R.J., 2017. Worldclim 2: New 1-km spatial resolution climate surfaces for global land areas. *Int. J. Climatol.* 37, 4302–4315. <https://doi.org/10.1002/joc.5086>. <http://worldclim.org/version2> (Accessed 29 Jul 2017).

Fischer, D., Thomas, S.M., Neteler, M., Tjaden, N.B., Beierkuhnlein, C., 2014. Climatic suitability of *Aedes albopictus* in Europe referring to climate change projections: Comparison of mechanistic and correlative niche modelling approaches. *Eur. Secur.* 19, 1–13. <https://doi.org/10.2807/1560-7917.ES2014.19.6.20696>.

Gubler, D.J., 2002. Epidemic dengue / dengue hemorrhagic fever as a public health, social and economic problem in the 21st century. *Trends Microbiol.* 10, 100–103.

Hartert, J., Ryan, S.J., MacKenzie, C.A., Parker, J.N., Strasser, C.A., 2013. Spatially explicit data: stewardship and ethical challenges in science. *PLoS Biol.* 11, e1001634.

Heydari, N., Larsen, D.A., Neira, M., Ayala, E.B., Fernandez, P., Adrian, J., Rochford, R., Stewart-Ibarra, A.M., 2017. Household dengue prevention interventions, expenditures, and barriers to *Aedes aegypti* control in Machala, Ecuador. *Int. J. Environ. Res. Public Health* 14, 196. <https://doi.org/10.3390/ijerph14020196>.

Ifaei, P., Karbassi, A., Jácome, G., Yoo, C.K., 2017. A systematic approach of bottom-up assessment methodology for an optimal design of hybrid solar/wind energy resources – Case study at middle east region. *Energy Convers. Manag.* 145, 138–157. <https://doi.org/10.1016/j.enconman.2017.04.097>.

INEC, 2010. *Censo de Población y Vivienda*. Instituto Nacional de Estadística y Censos.

IPCC, 2007. *General Guidelines on the Use of Scenario Data For Climate Impact and Adaptation Assessment*. WMO-UNEP, Helsinki, Finland.

Islam, T., 2012. Partial Least Square Regression Analysis to Investigate Climatic Dengue Risk Factors: A global study. Umeå University. <http://www.phmed.umu.se/>

digitalAssets/104/104551\_tasmia-islam.pdf (Accessed 20 July 2017).

Jácome, G., Valarezo, C., Yoo, C., 2018. Assessment of water quality monitoring for the optimal sensor placement in lake Yahuarcocha using pattern recognition techniques and geographical information systems. *Environ. Monit. Assess.* 190 (4). <https://doi.org/10.1007/s10661-018-6639-x>.

Johansson, M.A., Dominici, F., Glass, G.E., 2009. Local and global effects of climate on dengue transmission in Puerto Rico. *PLoS Neglect. Tropic Dis.* 3 (2), e382.

Johansson, E., Yahia, M.W., Arroyo, I., Bengs, C., 2017. Outdoor thermal comfort in public space in warm-humid Guayaquil, Ecuador. *Int. J. Biometeorol.* <https://doi.org/10.1007/s00484-017-1329-x>.

Karim, N., Munshi, S.U., Anwar, N., Alam, S., 2012. Climatic factors influencing dengue cases in Dhaka city: a model for dengue prediction. *Indian J. Med. Res.* 136, 32–39.

Khormi, H.M., Kumar, L., 2014. Climate change and the potential global distribution of *Aedes aegypti*: spatial modelling using geographical information system and CLIMEX. *Geospat. Health* 8 (2), 405–415.

Koch, L.K., Cunze, S., Werblow, A., Kochmann, J., Dörge, D.D., Mehlhorn, H., Klüppel, S., 2016. Modeling the habitat suitability for the arbovirus vector *Aedes albopictus* (Diptera: Culicidae) in Germany. *Parasitol. Res.* 115, 957. <https://doi.org/10.1007/s00436-015-4822-3>.

Kraemer, M., Sinka, M., Duda, K., Mylne, A., Shearer, F., Barker, C., et al., 2015. The global distribution of the arbovirus vectors *Aedes aegypti* and *Ae. Albopictus*. *eLifeXX* 4, e08347. <https://doi.org/10.7554/eLife.08347>.

Lee, K.Y., Chung, N., Hwang, S., 2016. Application of an artificial neural network (ANN) model for predicting mosquito abundances in urban areas. *Ecol. Inform.* 36, 172–180. <https://doi.org/10.1016/j.ecoinf.2015.08.011>.

Li, B., Morris, J., Martin, E.B., 2002. Model selection for partial least squares regression. *Chemom. Intell. Lab. Syst.* 64, 79–89.

Lippi, C.A., Stewart-Ibarra, A.M., Muñoz, Á.G., Borbor-Córdova, M.J., Mejía, R., Rivero, K., ... Ryan, S.J., 2018. The social and spatial ecology of dengue presence and burden during an outbreak in Guayaquil, Ecuador, 2012. *Int. J. Environ. Res. Public Health* 15, 827. <https://doi.org/10.3390/ijerph15040827>.

Lomax, R.G., Hahs-Vaughn, D.L., 2012. *An introduction to statistical concepts, 3<sup>rd</sup> ed.* Taylor & Francis Group, LLC, New York – London (ISBN 978-0-415-88005-3).

Masimalai, P., 2015. GIS for rapid epidemiological mapping and health-care management with special reference to filariasis in India. *Int. J. Med. Sci. Public Health* 4 (8). <https://doi.org/10.5455/ijmsph.2015.21072014213>.

Meltzer, M.I., Rigau-Perez, J.G., Clark, G.G., et al., 1998. Using disability-adjusted life years to assess the economic impact of dengue in Puerto Rico: 1984–1994. *Am. J. Trop. Med. Hyg.* 59, 265–271.

Ministerio de Salud de la Nación, 2013. *Enfermedades infecciosas: Dengue. Guía para el equipo de salud*. Ministerio de Salud de la Nación, Buenos Aires, Argentina.

Ministerio de Salud Pública del Ecuador, 2013. *Boletín epidemiológico del Dengue en el Ecuador*. MSP, Quito.

Moffett, A., Shackelford, N., Sarkar, S., 2007. Malaria in Africa: vector species' niche models and relative risk maps. *PLoS One* 2, e824.

Mondini, A., Chiaravalloti, F., 2008. Spatial correlation of incidence of dengue with socioeconomic, demographic and environmental variables in a brazilian city. *Sci. Total Environ.* 393, 241–248.

Montagner, F.R.G., Silva, O.S., Jahnke, S.M., 2018. Mosquito species occurrence in association with landscape composition in green urban areas. *Braz. J. Biol.* 78 (2), 233–239. <https://doi.org/10.1590/1519-6984.04416>.

Moya, W., Jacome, G., Yoo, C., 2017. Past, current, and future trends of red spiny lobster based on PCA with MaxEnt model in Galapagos Islands, Ecuador. *Ecolo. Evol.* 00, 1–10. <https://doi.org/10.1002/ece3.3054>.

Mulligan, K., Dixon, J., Joanna Sinn, C.L., Elliott, S.J., 2015. Is dengue a disease of poverty? A systematic review. *Pathog. Glob. Health* 109, 10–18.

Mweya, C.N., Kimera, S.I., Stanley, G., Misirzo, G., Mbobera, L.E.G., 2016. Climate change influences potential distribution of infected *aedes aegypti* co-occurrence with dengue epidemics risk areas in Tanzania. *PLoS One* 11 (9), e0162649. <https://doi.org/10.1371/journal.pone.0162649>.

OMS, 2009. *Dengue: Guías para el diagnóstico, tratamiento, prevención y control*. OPS/OMS, La Paz, Bolivia.

Pavez-Fox, M., Estay, S.A., 2016. Correspondence between the habitat of the threatened pudú (Cervidae) and the national protected area system of Chile. *BMC Ecol.* 16, 1–7. <https://doi.org/10.1186/s12898-015-0055-7>.

Phillips, S.J., Dudík, M., 2008. Modeling of species distributions with Maxent: new extensions and a comprehensive evaluation. *Ecography* 31, 161–175. <https://doi.org/10.1111/j.2007.0906-7590.05203.x>.

Phillips, S.J., Anderson, R.P., Schapire, R.E., 2006. Maximum entropy modeling of species geographic distributions. *Ecol. Model.* 190 (3–4), 231–259. <https://doi.org/10.1016/j.ecolmodel.2005.03.026>.

Phillips, S.J., Dudík, M., Schapire, R.E., 2017. *Maxent Software for Modeling Species Niches and Distributions* (Version 3.4.1). <http://biodiversityinformatics.amnh.org/open-source/maxent/>. (Accessed 26 May 2017).

Pourrut, P., 1983. Los climas del Ecuador: fundamentos explicativos. [http://horizon-documentation.ird.fr/exl-doc/pleins\\_textes/divers11-10/21848.pdf](http://horizon-documentation.ird.fr/exl-doc/pleins_textes/divers11-10/21848.pdf). (Accessed 15 Dec 2017).

Racloz, V., Ramsey, R., Tong, S., Hu, W., 2012. Surveillance of dengue fever virus: a review of epidemiological models and early warning systems. *PLoS Neglect. Tropic Dis.* 6 (5), e1648. <https://doi.org/10.1371/journal.pntd.0001648>.

Real-Cotto, J.J., 2017. Factores relacionados con la dinámica del dengue en Guayaquil, basado en tendencias climáticas históricas. *Anal. Facultad Medi.* 78 (1), 23–28. <https://doi.org/10.15381/anales.v78i1.13017>.

Real-Cotto, J.J., Regato-Arrata, M.E., Burgos-Yépez, V.E., Jurado-Cobeña, E.T., 2017. Evolución del virus dengue en el Ecuador. Período 2000 a 2015. *Anal. Facultad Medi.* 78 (1), 29–35. <https://doi.org/10.15381/anales.v78i1.13018>.

Real-Cotto, J.J., Briones-Lavayen, A., Decker-Yáñez, O., Hington-Chica, F., Jiménez-Vásquez, K., Vera-Lorenti, F., Faríño-Cortez, J., Cercado-Mancero, A., 2016. Estudio de clases de Dengue: DCSA y DG en pacientes ingresados en el hospital de Infectología de Guayaquil. Rev. Ciencia UNEMI 9 (1390–4272), 101–107.

Reiter, P., 2001. Climate change and mosquito-borne disease. Environ. Health Perspect. 109, 141–161.

Reiter, P., Lathrop, S., Bunning, M., Biggerstaff, B., Singer, D., Tiwari, T., et al., 2003. Texas lifestyle limits transmission of dengue virus. Emerg. Infect. Dis. 9, 86–89.

Sarfraz, M.S., Tripathi, N.K., Tipdecho, T., Thongbu, T., Kerdhong, P., Souris, M., 2012. Analyzing the spatio-temporal relationship between dengue vector larval density and land-use using factor analysis and spatial ring mapping. BMC Public Health 12 (1), 1–19. <https://doi.org/10.1186/1471-2458-12-853>.

SENPLADES, 2013. *National Plan of Good Living*, 1st ed. Secretaría Nacional de Planificación y Desarrollo - SENPLADES, Quito Available at: [www.planificacion.gob.ec](http://www.planificacion.gob.ec), Accessed date: 11 November 2017.

Stewart-Ibarra, A.M., Ryan, S.J., Beltrán, E., Mejía, R., Silva, M., Muñoz, A., 2013. Dengue vector dynamics (*Aedes aegypti*) influenced by climate and social factors in Ecuador: implications for targeted control. PLoS One 8 (11), e78263. <https://doi.org/10.1371/journal.pone.0078263>.

Stewart-Ibarra, A.M., Muñoz, Á.G., Ryan, S.J., Ayala, E.B., Borbor-Cordova, M.J., 2014. Spatiotemporal clustering, climate periodicity, and social-ecological risk factors for dengue during an outbreak in Machala, Ecuador, in 2010. BMC Infect. Dis. 14, 610. <https://doi.org/10.1186/s12879-014-0610-4>.

Teurlai, M., Menkès, C.E., Cavareiro, V., Degallier, N., Descloux, E., Grangeon, J.-P., et al., 2015. Socio-economic and climate factors associated with dengue fever spatial heterogeneity: a worked example in New Caledonia. PLoS Neglect. Tropic Dis. 9 (12), e0004211. <https://doi.org/10.1371/journal.pntd.0004211>.

Touhami, I., Haddag, H., Didi, M., Messadi, D., 2016. Contribution of modified harary index to predict Kováts retention indices for a set of PAHs. Chromatographia 79, 1023. <https://doi.org/10.1007/s10337-016-3120-2>.

Tu, J., Xia, Z.G., 2008. Examining spatially varying relationships between land use and water quality using geographically weighted regression I: model design and evaluation. Sci. Total Environ. 407, 358–378.

Van Benthem, B.H.B., Vanwambeke, S.O., Khantikul, N., Burghoorn-Maas, C., Panart, K., Oskam, L., et al., 2005. Spatial patterns of and risk factors for seropositivity for dengue infection. Am. J. Trop. Med. Hyg. 72, 201–208.

Vanwambeke, S., Van Benthem, B., Khantikul, N., Burghoorn-Maas, C., Panart, K., Oskam, L., Lambin, E., Sombroek, P., 2006. Multi-level analyses of spatial and temporal determinants for dengue infection. Int. J. Health Geogr. 5, 22.

Vanwambeke, S.O., Sombroek, P., Harbach, R.E., Isenstadt, M., Lambin, E.F., Walton, C., Butlin, R.K., 2007. Landscape and land cover factors influence the presence of *Aedes* and *Anopheles* larvae. J. Med. Entomol. 44 (1), 133–144.

Wen, T.-H., Lin, N.-H., Lin, C.-H., King, C.-C., Su, M.-D., 2006. Spatial mapping of temporal risk characteristics to improve environmental health risk identification: a case study of a dengue epidemic in Taiwan. Sci. Total Environ. 367, 631–640.

West, A.M., Kumar, S., Brown, C.S., Stohlgren, T.J., Bromberg, J., 2016. Field validation of an invasive species Maxent model. Ecol. Inform. 36, 126–134. <https://doi.org/10.1016/j.ecoinf.2016.11.001>.

WHO, 2009. Dengue: Guidelines for Diagnosis, Treatment, Prevention and Control. World Health Organization, Geneva, Switzerland.

WHO, 2012. Global Strategy for Dengue Prevention and Control 2012–2020. World Health Organization, Geneva.

Zhu, M., Lin, Z., 2018. The impact of human activity on the risk index and spatial spreading of dengue fever. Nonlinear Anal. Real World Appl. 39, 424–450. <https://doi.org/10.1016/j.nonrwa.2017.07.007>.